Soil-structure interaction analysis of lateral resistance of piles in liquefied and laterally spreading ground

Yung-Yen Ko[1] and J.-H. Hwang[2]

[1] Department of Civil Engineering, National Cheng Kung University, No.1, University Road, Tainan 70101, Taiwan
[2] Department of Civil Engineering, National Central University, No. 300, Zhongda Road, Taoyuan 32001, Taiwan

ABSTRACT

In this paper, the lateral resistance of piles subject to the actions of liquefaction-induced lateral spreading of the ground was investigated. The Winkler foundation model was utilized for the modeling of pile-soil interaction. The soil springs with nonlinear p-y curves were used to describe the relationship of soil reaction versus lateral displacement around the pile. The distributed plastic hinges were deployed to simulate the possible flexural failure of the pile. The actions due to lateral spreading of liquified ground were modeled as flow displacement and flow pressure, respectively. For the former, the free-field ground displacement profile is assigned to the pile-soil system; while the latter imposes the liquefaction-induced flow pressure directly on the pile. One of the pile failure cases due to lateral spreading of liquified ground in the 1995 Kobe Earthquake was adopted for case study. The obtained pile damage states from flow displacement and flow pressure methods were compared with the field observations, and the validity and feasibility of both methods were accordingly examined.

Keywords: soil-structure interaction; lateral resistance of piles; liquefaction; lateral spreading

1 INTRODUCTION

Piles are often designated to carry lateral loads, especially seismic loads. In addition to the inertia force transmitted from the superstructure, lateral spreading of liquefied ground also induces lateral load to piles during earthquakes, which is rather destructive to the piles for their being surrounded by soil. Usually the flexural failure is dominant because of the considerable bending moment generated by the lateral load, and for slender piles the buckling may occur due to the combination of axial load and lateral deflection, namely, the p-Δ effect (Bhattacharya and Madabhushi, 2013). Many cases have been reported, mostly related to foundations of structures near waterfront, such as bridges along or across rivers, or wharves, tanks and buildings in the port area.

Therefore, this study aims to investigate the lateral resistance of piles subject to the actions of laterally spreading ground triggered by liquefaction. The beam-on-Winkler's foundation model, in which soil reactions are modeled by spring elements along the pile, is utilized to represent the pile-soil interaction. Nonlinear p-y curves are used to describe the force-displacement relationship of the soil springs. The distributed plastic hinge method is adopted to simulate the possible flexural failure of piles. Thus, the nonlinear behavior of the pile-soil system can be well exhibited at a reasonable analysis cost. In engineering practice, the actions on piles due to the lateral spreading of the liquified ground are usually simulated by the flow displacement method, e.g. Ashford et al. (2011), as well as the flow pressure method, e.g. JRA (2012), and both will be introduced herein. In addition, a case study of pile failure caused by lateral spreading in the 1995 Kobe Earthquake using both methods will be presented. Their feasibility and validity will be discussed as the reference of the seismic performance assessment of piles in liquefiable ground.

2 PILE DAMAGE DUE TO LATERAL SPREADING OF LIQUEFIED GROUND

2.1 Liquefaction-induced lateral spreading

During earthquakes, finite lateral displacement of gently sloping ground underlain by loose sands with a shallow groundwater table may occur due to the build-up of excess pore pressure or even liquefaction in the underlying deposit, as shown in Fig 1(a) (Rauch, 1997). This is often called the lateral spreading of liquefied ground. Gently sloping means a slope less than 6%, or the flow failure may occur. (Youd, 1995). A steep free face giving an unrestricted boundary, e.g. riverbank or seashore, is common in lateral spreading.

The profile of laterally spreading ground is shown in Fig. 1(b), which can be divided into a non-liquefied (unsaturated, impervious or clayey) top layer (so-called crust layer) and a liquefied (saturated, loose and sandy) underlying layer. Tension cracks or ground fissures perpendicular to the direction of spreading as well as slumping are often found on the ground surface, especially near the upper margins of the spreading area.

2.2 Cases of pile damage related to lateral spreading

In the 1964 Niigata Earthquake, soil liquefaction and its devastating effects started to catch the attention of

engineers. Because the lateral spreading induced permanent ground displacement, a public building suffered flexural failure of piles which concentrated at the interface of the liquefied and non-liquefied layers, and piles moved by non-liquefied soil layers were worse damaged (Dobry et al., 2003). The Showa Bridge collapsed possibly due to the combined effect of axial load and lateral spreading which leaded to buckling instability of piles (Bhattacharya and Tokimatsu, 2013).

The 1995 Kobe Earthquake brought severe damages to the Port of Kobe because of liquefaction, and therefore several facilities experienced pile failure caused by lateral spreading. In a pile-supported wharf, a horizontal displacement up to 1.7 m at the deck and local buckling of the steel pipe piles associated with significant lateral deformation of the sand layer were observed (PIANC, 2001). The seaward movement of a quay wall damaged the precast concrete (PC) piles of a nearby oil-storage tank in terms of lateral deformation and flexural cracks, which were more severe near the interface of the liquefied fill deposit and underlying silty soil layer (Ishihara and Cubrinovski, 2004).The PC piles of a building near the waterfront were severely cracked and even broken due to a displacement above 1.5 m of the quay wall, which leaded to considerable tilting of the superstructure (Tokimatsu et al., 1997).

A recent case was reported in the 2016 Kaikoura, New Zealand Earthquake, that a lateral spreading with a displacement of 0.8-1.0 m at the edge of the fill pushed a pile-supported wharf to a tilt of 1-2.5° and a seaward moment of 0.2-0.5 m (Cubrinovski et al., 2017).

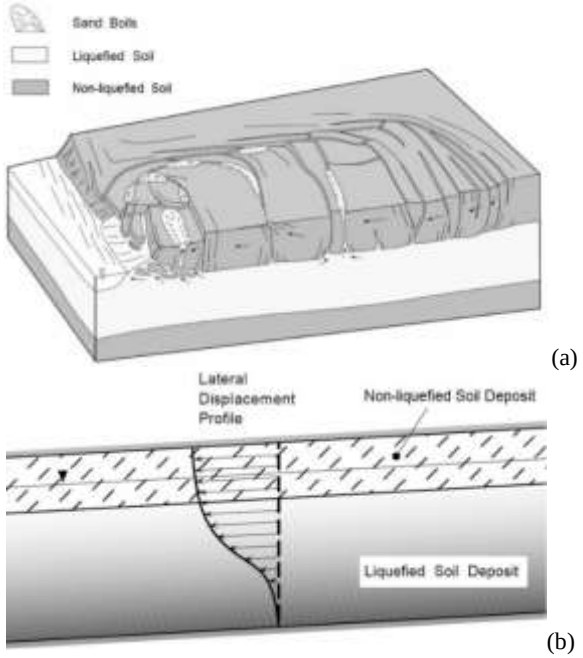

Fig. 1. Liquefaction-induced lateral spreading: (a) schematic depiction; (b) lateral displacement profile. (after Rauch (1997))

3 MODELLING OF ACTIONS OF LATERAL SPREADING ON PILE

Fig. 2(a) shows the typical condition of the lateral spreading of liquefied ground acting on the pile. The moving soil body leans against the pile; meanwhile, the soil reaction to provide lateral resistance of the pile is reduced due to liquefaction. Large flexural deformation and bending moment of the pile may be thus caused. Lateral spreading is even damaging if a non-liquefied layer is on the top of moving soil. Two methods for the modelling of these actions are introduced as follows.

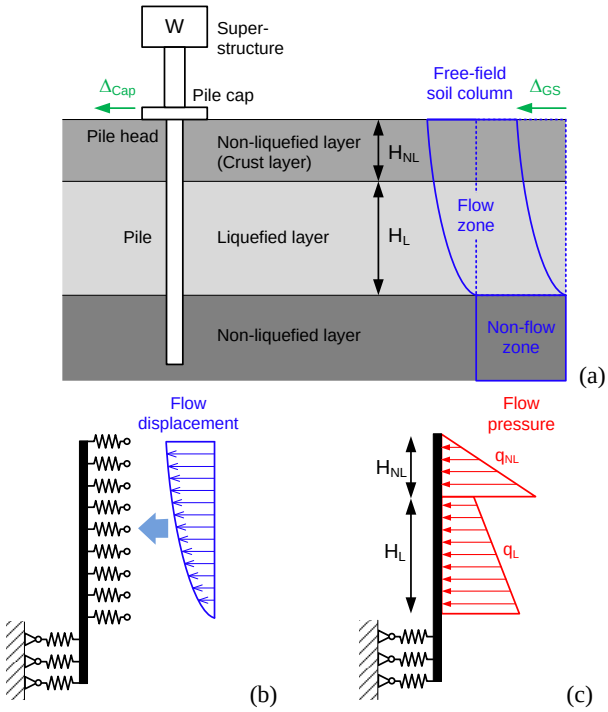

Fig. 2. Actions of lateral spreading on pile and its modelling: (a) typical condition in the field; (b) flow displacement method; (c) flow pressure method.

3.1 Flow displacement method

Firstly, the free-field ground displacements profile due to lateral spreading is estimated, e.g. Tokimatsu and Asaka (1998). Then, the displacement profile is assigned as the boundary conditions to the support ends of the soil springs, as shown in Fig. 2(b). It might be necessary to reduce the subgrade reaction coefficients or the p-y curves of the soil springs based on the liquefaction potential of the corresponding soil layers.

3.2 Flow pressure method

As shown in Fig. 2(c), the actions of lateral spreading are represented by flow pressure directly imposed on the pile. The flow pressure profile in the non-liquefied layer with respect to the depth x, $q_{NL}(x)$, and that in the liquefied layer, $q_L(x)$, are given as (JRA, 2012):

$$q_{NL}(x) = c_s c_{NL} K_P \gamma_{NL} x \quad \text{for } 0 \le x \le H_{NL} \qquad (1)$$

$$q_{NL}(x) = c_s c_L [\gamma_{NL} H_{NL} + \gamma_L (x - H_{NL})]$$

$$\text{for } H_{NL} < x \le H_{NL} + H_L \qquad (2)$$

where K_P is the passive earth pressure coefficient; c_L is the modification factor for flow pressure in the liquefied layer, which is suggested to be 0.3, while that in the non-liquefied layer, c_{NL}, is based on the liquefaction potential index (P_L); c_s is the modification factor based on the distance to the waterfront. Suggested values of c_{NL} and c_s are listed in Table 1. It is noted that the flow zone in Fig. 2(a) induces flow pressure but provides no soil reaction, while the non-flow zone induces no flow pressure but provides soil reaction.

Table 1. Modification factors for flow pressure

P_L	c_{NL}	Distance to waterfront, s (m)	c_s
$P_L \le 5$	0	$s \le 50$	1.0
$5 < P_L \le 20$	(0.2 P_L - 1)/3	$50 < s \le 100$	0.5
$20 < P_L$	1	$100 < s$	0

4 CASE STUDY

4.1 Case introduction

A building near the waterfront suffered pile damage due to liquefaction-induced lateral spreading during the 1995 Kobe Earthquake, as mentioned in Section 2.2 and as shown in Fig. 3, was adopted for case study. The quay wall nearby moved seaward about 1.6 m, and a ground surface displacement around 0.8~1.0 m was observed at the base of the building. Horizontal and longitudinal cracks were caused at the pile head and near the interface between the reclaimed fill and the underlying sand layer, and one pile at the sea side was even broken at its upper part. The superstructure was therefore tilted about 3 degrees. Based on the boring data of the site (Tokimatsu et al., 1997) and a recoded PGA of about 0.3g, the liquefaction potential was assessed using the procedure proposed by AIJ (2001). The results indicate that the upmost non-liquefied layer with a thickness about 2 m was underlain by a 7 m thick liquefied layer, and below the depth of 9 m is the lower non-liquefied layer.

4.2 Analysis model and conditions

Fig. 4 show the analysis model of pile S-7 and pile N-7 in Fig. 2 generated by the software SAP2000. The Winkler's foundation model is utilized for the modeling of pile-soil interaction, that is, the pile is modeled by beam elements and the soil reactions are modeled by spring elements deployed along the pile. Nonlinear p-y curves for the soil springs are used to represent the nonlinearity of supporting soil. A rigid body constraint was specified to both pile caps to approximate the connection provided by the grade beam. To simulate the possible flexural failure of piles, the distributed plastic hinge method is adopted, which inserts multiple plastic hinges along the expected plastic zone of a structural member. This is because the location of the maximum moment along a laterally loaded pile may vary with the plasticity development of the surrounding soil (Chiou et al., 2009). Thus, the nonlinear behavior of the pile-soil system can be well captured at a reasonable analysis cost.

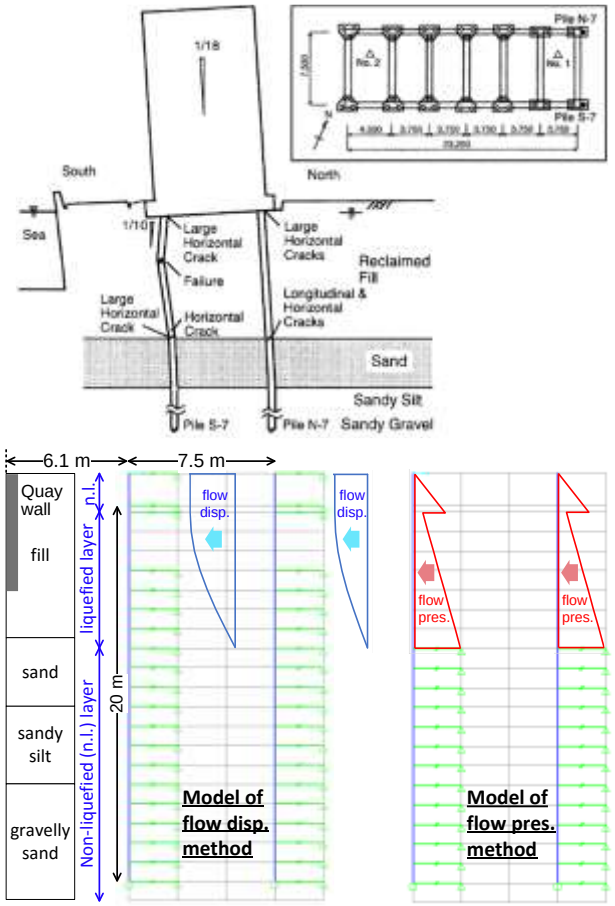

Fig. 3. Pile damage of a building near waterfront during 1995 Kobe Earthquake and its SAP2000 model.

The p-y curves were specified using both the SPT-N based subgrade reaction coefficient in JRA (2012) and the nonlinear secant modulus in AIJ (2001), and were further reduced according to AIJ (2001) considering the degradation of liquefied soil. Noting that the soil reaction was reduced to zero between the depth of 2~5 m.

The moment-curvature relationship of the plastic hinge was given based on Uzuoka et al. (2002), where the crack moment M_{cr}= 63.7 kN-m, ultimate moment M_u= 133.3 kN-m and yielding moment $M_y = 0.85M_u$. The section rigidity EI after cracking is reduced to 1/5 of the initial one, and is reduced to 1/100 after yielding.

For the flow displacement method, the displacement profile d_{ls} is depicted as (Tokimatsu and Asaka, 1998):

$$\begin{cases} d_{ls}(z,x) = D_0\left(\frac{1}{2}\right)^{5x/L} & \text{for } 0 \le z < z_w \\ d_{ls}(z,x) = D_0\left(\frac{1}{2}\right)^{\frac{5x}{L}} \cos\left[\frac{\pi(z-z_w)}{2H}\right] & \text{for } z \ge z_w \end{cases} \qquad (3)$$

where $D(x)$ is the ground surface displacement at a distance of x from waterfront; D_0 denotes $D(x=0)$, L is the length of the laterally spreading area and $L =$

$50D_0$ can be regarded as a representative. z is the depth below the ground surface, z_w is the depth at the top, and H is the thickness of the liquefied layer. In this case, D_0 = 1.6 m, z_w = 2 m and H = 9 m.

4.3 Analysis results

Fig 4 shows the pile deformation and development of plastic hinges obtained by the flow displacement method. When only the actions of the lateral spreading were considered, the displacement of pile cap was 0.9 m, conforming to the field observations. Plastic hinges occurred near the pile head and below the interface of non-liquefied and liquefied layers, and yielding state was reached at the pile head and a depth around 10~11 m, close to the real situation. Further including the axial load from superstructure, the piles reached the ultimate state when 70% of the prescribed displacement profile was imposed. The P-Δ effect of the axial load might worse the flexural damage of the pile. It is noted that the breaking of the pile at a depth of 4~5 m, where the soil reaction was reduced to zero due to liquefaction, was not reproduced. The absence of lateral confinement might cause the geometric instability (buckling) of the pile, which was probably not well simulated by the analysis.

The results of flow pressure method are depicted in Fig 6. The damage locations were similar, but the ultimate state was reached when 70% of the pressure was applied with a wider damage range for no axial load case, which means this method is relatively conservative. If the axial load was included, no convergence solution can be obtained before the ultimate state. It is possibly due to the buckling occurred prior to the flexural failure because the pile had no lateral confinement in its upper part yet was both laterally and axial loaded.

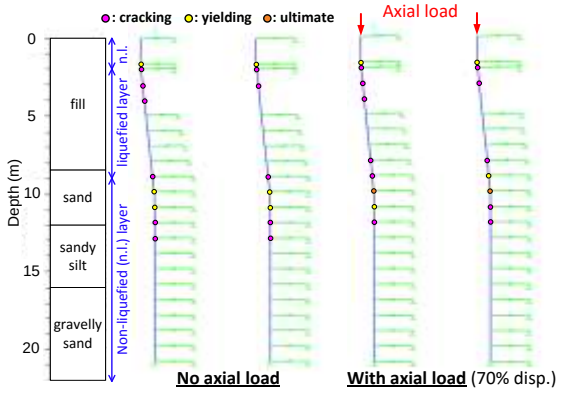

Fig. 4. Results of flow displacement methods.

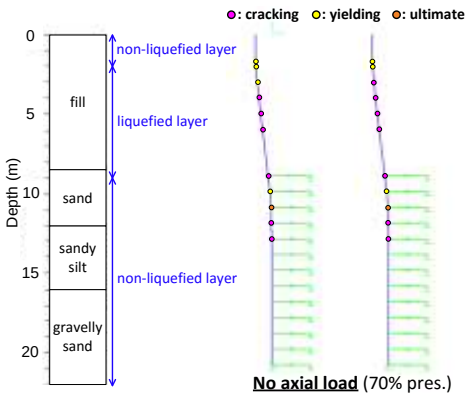

Fig. 5. Results of flow pressure method.

5 CONCLUSION

(1) Both flow displacement and flow pressure methods can predict the locations of flexural failure of piles subjected to the actions of liquefaction-induced lateral spreading of the ground.

(2) The pile displacement and damage state estimated by flow displacement method based on the ground displacement profile proposed by Tokimatsu and Asaka (1998) are close to the field observations, while the flow pressure method based on the pressure profile proposed by JRA (2012) gave conservative results.

(3) For a pile in laterally spreading ground, the axial load from the superstructure significantly intensifies the flexural failure and leads to buckling instability concerns as well. Thus, the effect of axial load should be considered in the seismic evaluation of piles.

REFERENCES

AIJ (Architectural Institute of Japan). (2001). Recommendations for design of building foundations, Tokyo (in Japanese)

Ashford, S.A., Boulanger, R.W., Brandenberg, S.J. (2011). Recommended Design Practice for Pile Foundations in Laterally Spreading Ground, PEER, Berkeley, CA.

Bhattacharya, S., Tokimatsu, K. (2013). Collapse of Showa Bridge revisited. International Journal of Geoengineering Case Histories, 3(1), 24-35.

Chiou, J.S., Yang, H.H., Chen, C.H. (2009). Use of plastic hinge model in nonlinear pushover analysis of a pile, Journal of Geotechnical and Geoenvironmental Engineering, 135(9), 1341-1346.

Dobry, R., Abdoun,, T., O'Rourke, T.D., Goh, S.H. (2003). Single piles in lateral spreads: field bending moment evaluation Journal of Geotechnical and Geoenvironmental Engineering, 129(10), 879-889.

Ishihara, K., Cubrinovski, M. (2004). Case studies of pile foundations undergoing lateral spreading in liquefied deposits, 5th International Conference on Case Histories in Geotechnical Engineering, New York, NY.

JRA (2012). Specifications for Highway Bridges, Part V–Seismic Design, Japan Road Association, Tokyo, Japan.

PIANC (World Association for Waterborne Transport Infrastructure) (2001). Seismic Design Guidelines for Port structures, A.A. Balkema Publishers, Lisse, Netherlands.

Rauch, A.F. (1997). EPOLLS: An Empirical Method for Predicting Surface Displacements Due to Liquefaction-Induced Lateral Spreading in Earthquakes, Ph.D. dissertation,

Virginia Polytechnic Institute and State University, VA.

Tokimatsu, K., Asaka, Y. (1998). Effects of liquefaction-induced ground displacements on pile performance in the 1995 Hyogoken-Nambu Earthquake, Soil and Foundations, Special Issue, 163-177.

Tokimatsu, K., Oh-oka, H., Ahamoto, Y., Asaka, Y. (1997). Failure and deformation modes of piles due to liquefaction- induced lateral spreading in 1995 Hyogoken-Nambu Earthquake, Journal of Structural and Construction Engineering, AIJ, 62(495), 95-100 (in Japanese).

Uzuoka, R., Sento, N., Yashima A., Zhang F. (2002). 3-dimensional effective stress analysis of a damaged group-pile foundation adjacent to a quay wall, JAEE Journal, 2(2), 1-14.

Youd, T.L. (1995). liquefaction-induced lateral ground displacement. 3rd International Conference on Recent Advances in Geotechnical Earthquake Engineering and Soil Dynamics, St. Louis, MS.